VIBRATION CONTROL OF GIRDER BRIDGE STRUCTURES THROUGH THE IMPLEMENTATION OF SUPERELASTIC SHAPE MEMORY ALLOY SPRINGS

Filipe Oliveira Damasceno[1]

Antônio Almeida Silva[1]

Armando Wilmans Nunes da Fonseca Júnior[1]

filipeo.damasceno@hotmail.com

antonio.almeida@ufcg.edu.br

armandowjunior@gmail.com

[1]Federal Universityof Campina Grande

Aprígio Veloso, 882, Universitário, 58429-900, Campina Grande, Paraíba, Brazil.

Abstract.*Every time the natural frequency of a machine or structure coincides with a vibration frequency of an external excitation, resonance appears and it can cause serious problems in civil constructions. Hence, it is important to control the latter. In this field the shape memory alloys (SMA) are gaining more and more usage due to its properties and ability to serve as a passive element of energy dissipation. This work has as an objective the vibration control in a girder bridge structure through the implementation of superelastic shape memory alloy springs. The mathematical model was based in a beam element fixed at one end and simply supported at the other with the springs attached to one point at the beam span. The experiments were realized with a shaker applying a transversal harmonic force at the bridge. It was noted that the damping ratio increased, causing a reduction of the vibration amplitude of the structure.*

Keywords:*Vibration, Energy dissipation,Shape memory alloys,Girder Bridges.*

1. INTRODUCTION

In a day to day basis it is easy to observe the presence of mechanical vibrations; they are all around the world. In some cases vibrations are desired, as in a guitar string. However, this phenomenon may have destructible effects. Every time the natural frequency of a machine or structure coincides with a vibration frequency of an external excitation, resonance appears and it can cause serious problems in civil construction, causing rupture of support beams due to the significant increase of vibration amplitude of the structure. Hence it is important to control the latter. In this field the shape memory alloys (SMA) are gaining more and more usage due to its two main properties: the shape memory effect and the superelasticity, which are used in active and passive vibration control, respectively. Recent studies gives a review of applications of Shape Memory Alloys. Recent studies, Alamet. al. (2007) e Jani et. al. (2014), shows a great potential for the application of shape memory alloys in several areas, such as civil construction, automotive, biomedicine and aerospace industries.

Some recent studies of bridges attenuation are referenced, as the study conducted by Liu et. al. (2016), that presents the implementation of these alloys to reduce the lateral and torsional vibrations of a bridge, considering only the free vibration of the latter. Hamdan and Jubran (1991) made a fairly precise mathematical model for this type of application when considering the addition of a concentrated mass along the bridge. Moraes (2017) developed a new concept of spring association in tendons to verify the effectiveness of the implementation of the SMA springs in a two-degree-of-freedom model simulating a two-store building. The results showed that about 60% of attenuation was possible in terms of displacements in the first mode of vibration.

2. METHODOLOGY

2.1. Forced damped vibration in a beam with concentrated mass

Figure 1 presents the model of the physical system used, which consists of an aluminum plate fixed at one end and simply supported at the other.

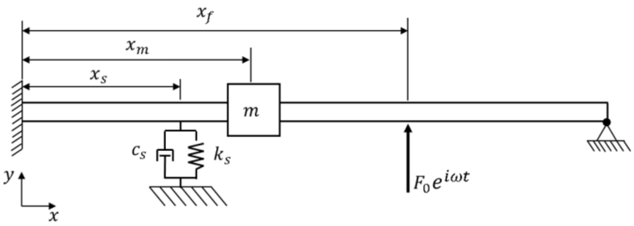

Figure 1–Bridge model

According to Liu et. al. (2016) and Hamdan & Jubran (1991)Eq. (1) presents the mathematical model in forced vibration, where m is the concentrated mass along the structure span, ρA is the linear density, EI presents the system stiffness, c is the equivalent viscous structural damping, c_s and k_s are viscous damping and stiffness constants of the SMA, respectively and $\delta(x - x_0)$ is Dirac delta function.

$$[\rho A + \delta(x - x_m)m]\frac{\partial^2 y(x,t)}{\partial t^2} + EI\frac{\partial^4 y(x,t)}{\partial x^4} + c\frac{\partial y(x,t)}{\partial t} + \delta(x - x_s)\left[k_s y(x,t) + c_s\frac{\partial y(x,t)}{\partial t}\right] = \delta(x - x_f)F_0 e^{i\omega t} \quad (1)$$

This equation has as solution:

$$y(x,t) = \sum_{n=1}^{\infty} \phi_n(x) q_n(t). \quad (2)$$

Where $q_n(t)$ is the generalized coordinate and $\phi_n(x)$ is the corresponding mode shape. Applying the particular solution at Eq. (1), multiplying by $\phi_n(x)$ and integrating along the beam we may find the differential equation at the generalized coordinate. The solution may be approximated as a system with 2 degrees of freedom using the matrix method. Hence the Eq. (1) may be simplified as:

$$[M]\{\ddot{q_n}(t)\} + [C]\{\dot{q_n}(t)\} + [K]\{q_n(t)\} = [Q]\{\mathrm{f(t)}\} \quad (3)$$

Where the matrices may be organized as:

- $M_{ii} = \rho A \int_0^l \phi_i^2(x)dx + m\phi_i^2(x_m)$
- $M_{ij} = m\phi_i(x_m)\phi_j(x_m)$
- $C_{ii} = c\int_0^l \phi_i^2(x)dx + c_s\phi_i^2(x_s)$
- $C_{ij} = c_s\phi_i(x_s)\phi_j(x_s)$
- $K_{ii} = EI\int_0^l \left[\frac{\partial^2\phi_i(x)}{\partial x^2}\right]^2 dx + k_s\phi_i^2(x_s)$
- $K_{ij} = k_s\phi_i(x_s)\phi_j(x_s)$
- $Q_i = \phi_i(x_f)F_0$

Since the excitation force is of the harmonic type, the response will be presenting the same behavior. The amplitude responses in Eq. (4) may be obtained using the impedance matrix of the system.

$$X_1(i\omega) = \frac{Z_{22}(i\omega)F_{10} - Z_{12}(i\omega)F_{20}}{Z_{11}(i\omega)Z_{22}(i\omega) - Z_{12}^2(i\omega)}; X_2(i\omega) = \frac{-Z_{12}(i\omega)F_{10} + Z_{11}(i\omega)F_{20}}{Z_{11}(i\omega)Z_{22}(i\omega) - Z_{12}^2(i\omega)} \quad (4)$$

Where:

$$[Z(i\omega)] = \begin{bmatrix} Z_{11}(i\omega) & Z_{12}(i\omega) \\ Z_{12}(i\omega) & Z_{22}(i\omega) \end{bmatrix} = \begin{bmatrix} -\omega^2 m_{11} + i\omega c_{11} + k_{11} & -\omega^2 m_{12} + i\omega c_{12} + k_{12} \\ -\omega^2 m_{12} + i\omega c_{12} + k_{12} & -\omega^2 m_{22} + i\omega c_{22} + k_{22} \end{bmatrix} \quad (5)$$

$\boldsymbol{F_{10}}$and$\boldsymbol{F_{20}}$ are the external forces acting on the system in each mode of vibration. $\boldsymbol{Z(i\omega)}$ is the impedance matrix and can be calculated in Eq. (5), the index numbered refers to the positions elements in the matrix. Those equations were used to obtain the analytical parameters in order to compare to the experimental ones.

2.2. Experimental model of the structure

The structural model adopted in this paper can be characterized in the Figure 2a, where a semi-crimped beam represents the bridge and the mass m is a concentrated charge which is fixed to the SMA device. It may be observed how the experiment was realized, with *M* is the counterweight used to act as a preload to the SMA spring. Fig. 2b show the two analytical mode shapes of the structure and the maximum deflection points, at where the absorber element, mass and measuring instrument were placed.

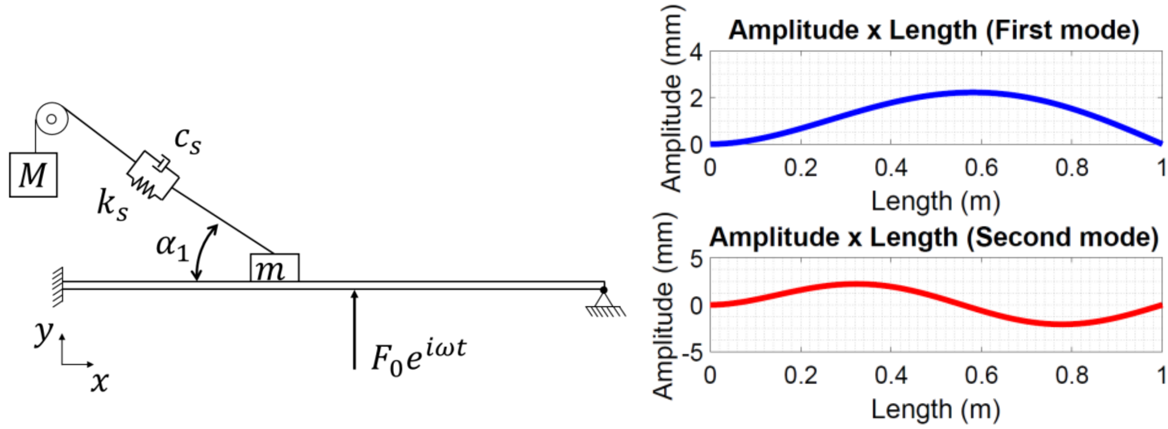

(a) (b)

Figure 2 – (a) Experimental model, (b) Mode shapes.

Table 1 shows the characteristics of the experimental model. According to Hamdan & Jubran (1991) $\beta_1 l$ and $\beta_2 l$ are frequency parameters used to calculate the natural frequencies of the structure, that can be found by solving of the transcendental equation of the mode shape.

Table 1 – Parameters used in the modeling.

Parameter	*Values*	*Parameter*	*Values*
Bridge length	1000 mm	**Young's modulus (E)**	71.0 GPa
Bridge density (ρ)	2770.0 kg/m³	$\boldsymbol{\beta_1 l}$	3.926602
Bridge thickness	3.175 mm	$\boldsymbol{\beta_2 l}$	7.068583
Bridge width	101.6 mm	**Mass**	126.95 g

2.3. Dynamic absorber selection

To select the mini-springs it was important to know how much deformation they could endure as a function of the vertical deflection of the bridge. The SMA mini-springs present a hysteretic loop when subjected to load and unload. Choosing a NiTi superelastic mini-spring used in odontological application and some results obtained by Grassi (2014), the maximum value of dissipated energy is between 80 and 500% of linear deformation. Hence it is necessary that the effective displacement of the absorbers is in this interval. It is possible to find the linearized stiffness of the springs between the 80 and 500% deformation to calculate the necessary pre-load. The useful length of 2.5 mm was chosen due to the largest loop formed.

As a way of comparing and evaluating only the amplitude reduction caused by the SMA absorbers, it was necessary to use steel springs with an equivalent stiffness. The tests were done using the steel and SMA springs separately.

3. RESULTS AND DISCUSSIONS

3.1. Results of forced vibration

With the results of forced vibration it was possible to calculate the reduction of the vibration amplitude when the system is in its critical condition, at resonance. According to Rao (2011) the damping ratios may be calculated utilizing the bandwidth method.

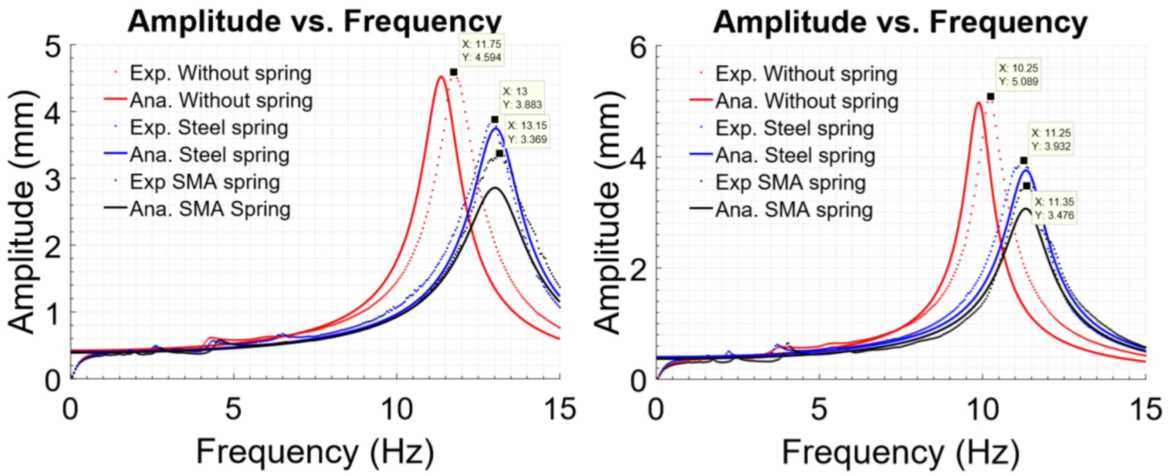

(a) (b)

Figure 3 – Superposed analytic and experimental graphs of forced vibration (a) Without mass; (b) With concentrated mass.

Table 2–Damping ratio and Vibration amplitudes

	Damping ratio			Experimental amplitude (mm)		
	No spring	**Steel Spring**	**SMA Spring**	**No Spring**	**Steel Spring**	**SMA Spring**
Without mass	0.0481	0.0555	0.0708	4.594	3.883	3.369
With mass	0.0404	0.0550	0.0616	5.089	3.932	3.476

Table 2 presents a summary of the damping values obtained (from Fig. 3), where it is possible to observe that the damping ratio was increased with the use of SMA springs. For the structure with the concentrated mass, there was a 27% increase in comparison to the steel springs and 47% increase in comparison to non-springs. With the concentrated mass, there was a 12% and 52%, respectively.

With regard to the vibration amplitudes at the resonance region, summarized in Table 2, there was a reduction of approximately 13% using SMA springs in comparison to the steel ones. Table 3 shows the comparison between the analytical and experimental natural damped frequencies of the bridge in all studied cases.

Table 3 – Natural frequencies of the bridge and relative error.

		ω_dExperimental (Hz)	**ω_dAnalytical (Hz)**	**Error (%)**	**Frequency reduction (%)**	
Without mass	Without spring	11.75	11.35	3.52%	-	-
	Steel spring	13.00	13.05	0.38%	-	-
	SMA Spring	13.15	13.00	1.15%	-	-
With mass	Without spring	10.25	9.90	3.54%	12.77%	12.78%
	Steel spring	11.25	11.35	0.88%	13.46%	13.03%
	SMA Spring	11.40	11.30	0.88%	13.31%	13.08%

Proceedings of the XXXVIII Iberian Latin-American Congress on Computational Methods in Engineering
P.O. Faria, R.H. Lopez, L.F.F. Miguel, W.J.S. Gomes, M. Noronha (Editores), ABMEC, Florianópolis, SC, Brazil, November 5-8, 2017.

Where it may be seen that the largest error was of 3.5% for the no spring configuration. It also may be seen that an added mass to the structure results in a large shift in its natural frequency (of 13.7%), hence making more crucial the use of adaptive dampers.

4. CONCLUSIONS

With regard to the amplitude reduction after the implementation of the designed device, which incorporates SMA springs as an energy dissipating element, it was possible to conclude that it happened only due to the hysteretic damping effect, since the structures had the same equivalent stiffness. This reduction wasn't larger because the resonance region was at a high frequency and the SMA springs lose its capacity of dissipating energy. The vibration amplitudes of the bridge were another hindrance, the ideal strain of the springs as a function of the bridge deformation was of 500%, however it was only possible to reach a 242.5% deformation due to structure and equipment limitations.

The analytical model had a good approximation, since the natural frequency errors were low. The errors of the vibration amplitudes were in major part due to the use of the bandwidth method, which is generally used in systems with low damping ratios.

ACKNOWLEDGMENT

The opportunity to participate in the PIBIC/CNPq-UFCG program; to advisor professor Antônio Almeida Silva; to Yuri Moraes for providing the data of his master's thesis.The Graduate Program in Mechanical Engineering of Federal University of Campina Grande (UFCG), and CNPq Brazilian research agency for funding the project Universal (Grant 444039/2014-7)

REFERENCES

Alam, M.; Youssef, M.; Nehdi, M. Utilizing shape memory alloys to enhance the performance and safety of civil infrastructure: a review**.** Can. J. Civ. Eng., Vol. 34. p. 1075–1086. 2007.

Grassi, E. N. D. *Comportamento Termomecânico de Minimolas Superelásticas de NiTi: Influência de Tratamentos Térmicos*. Campina Grande, PB: UFCG, 2014. 115 p. Master's Thesis, Federal University of Campina Grande, 2014.

Hamdan, M. N.; Jubran, B. A. *Free and Forced Vibrations of a Restrained Cantilever Beam Carrying a Concentrated Mass*. J KAU: Eng. Sci., vol. 3, Pg. 71-83.1991.

Jani, J. M.; Leary, M.; Subic, A. Gibson, M. A. *A review of shape memory alloy research, applications and opportunities*. Materialsand Design, Vol. 56, p. 1078-113. 2014.

Lagoudas, D. C.; Mayes, J. J.; Khan, M. M. Simplified Shape Memory Alloy (SMA) Model for Vibration Isolation. Smart Structures and Materials: Modeling, Signal Processing, and Control in Smart Structures, v. 452, Aug. 2001.

Liu, A. R.; Liu, C. H.; Fu, J. Y.; Pi, Y. L.; Huang, Y. H.; Zhang, J. P. *A Method of Reinforcement and Vibration Reduction of Girder Bridges Using Shape Memory Alloy*

Cables. International Journal of Structural Stability and Dynamics. World Scientific Publishing Company. Vol. 17. No. 7. Septemberof 2016.

Moraes, Y. J. O. *Análise Dinâmica Aplicada ao Controle Passivo de Vibrações em Estrutura do Tipo Pórtico Incorporando Minimolas Superelásticas de Nitinol*. Campina Grande, PB. 114p. Master'sThesis – PPGEM/UAEM, Federal Universityof Campina Grande, 2017.

Rao, S. S. *Vibrações Mecânicas.*4th Ed. São Paulo: Pearson Prentice Hall, 2011.